

EPR investigation of the electronic states in β' -type $[\text{Pd}(\text{dmit})_2]_2$ compounds (where dmit is 2-thioxo-1,3-dithiole-4,5-dithiolate)

Toshikazu Nakamura,^{a,b} Toshihiro Takahashi,^b Shuji Aonuma^c and Reizo Kato^{c,d}

^aInstitute for Molecular Science, Myodaiji, Okazaki, 444-8585, Japan.

E-mail: t-nk@ims.ac.jp

^bDepartment of Physics, Gakushuin University, Mejiro 1-5-1, Toshima-ku, Tokyo, 171-8588, Japan

^cThe University of Tokyo, Roppongi, Tokyo, 106-8666, Japan

^dThe Institute of Physics and Chemical Research, 2-1 Hirosawa, Wako-shi, Saitama, 351-0198, Japan

Received 2nd March 2001, Accepted 6th April 2001

First published as an Advance Article on the web 4th May 2001

Magnetic investigations of organic conductors, β' -type $[\text{Pd}(\text{dmit})_2]_2$, have been performed by Electron Paramagnetic Resonance (EPR) measurements. We found that most of them except one compound underwent antiferromagnetic transitions. Although they are isostructural with little differences in lattice parameters, their spin–spin correlations and antiferromagnetic transition temperatures show strong counter ion dependence. The EPR g -values of $\text{Pd}(\text{dmit})_2$ cannot be explained within the framework of isolated radical description which is a good approximation for conventional organic conductors. The electronic structures of a series of molecular conductors based on $\text{Pd}(\text{dmit})_2$ at ambient pressure are discussed from microscopic points of view.

Research on metal dithiolene complexes $\text{M}(\text{dmit})_2$, where dmit (C_3S_5) is 2-thioxo-1,3-dithiole-4,5-dithiolate, is one of the major trends in the development of organic conductors with new functions. Although several metallic phases are found in $\text{Ni}(\text{dmit})_2$ compounds even at ambient pressure,¹ most $\text{Pd}(\text{dmit})_2$ compounds (especially the β' -type one) are paramagnetic insulators at ambient pressure.^{2,3} Since the crystal structure of the $\text{Pd}(\text{dmit})_2$ system is based on stacks of strongly dimerized $\text{Pd}(\text{dmit})_2$ molecules, the energy levels of the antibonding HOMO band become higher than those of the bonding LUMO.⁴ As a result, it is considered that the conduction band is formed by the two-dimensional half-filled HOMO band. Although the mechanism of the charge localization of β' -type $\text{Pd}(\text{dmit})_2$ compounds has not been clear, the above consideration suggests that the non-metallic state at ambient pressure is a Mott–Hubbard insulator. In previous ¹H-NMR measurements on the analogous $\text{Pd}(\text{dmise})_2$ based compounds, where dmise ($\text{C}_3\text{S}_4\text{Se}$, 2-selenoxo-1,3-dithiole-4,5-dithiolate) is one of the selenium-containing analogues of dmit, we found that they underwent antiferromagnetic transitions.⁵ The large local magnetization in antiferromagnetic states ruled out the possibility of spin-density wave (SDW) formations originating from Fermi surface instability. Hence we concluded that the electronic state at ambient pressure of this family should be understood as a Mott–Hubbard insulator rather than a correlated metal. However, some problems remain unsolved; for several $\text{Pd}(\text{dmit})_2$ compounds, the local magnetizations in the antiferromagnetic states are very small.⁶ The absolute value of the local magnetization and transition temperatures, T_N 's, are different between $\text{Pd}(\text{dmit})_2$ and $\text{Pd}(\text{dmise})_2$ based compounds.

The main aim of this study is to determine the antiferromagnetic state and to clarify the electronic states by systematic investigations of $\text{Pd}(\text{dmit})_2$ compounds. We performed EPR measurements for an isostructural series of β' - $\text{Et}_2\text{Me}_2\text{Z}$ and $\text{Me}_4\text{Z}[\text{Pd}(\text{dmit})_2]_2$ (Me = methyl; Et = ethyl; Z = P, As, Sb). The T_N , the principal values and axes of the EPR g -tensor were

determined. We discuss the electronic states of $[\text{Pd}(\text{dmit})_2]_2$ as a strong dimer system.

Experimental

Sample preparation and crystal structural data were previously reported.^{3,7–9} The EPR measurements were carried out for 1–10 aligned single crystal(s) using an X-band spectrometer JES-FE3XG (JEOL) (with a cylindrical cavity: TE_{011}) equipped with an Air Products continuous-flow cryostat LTR-3. The temperature range of the EPR measurements was between 100 and 7 K. At high temperatures, it is hard to obtain reliable EPR spectra because of the line broadening. Temperature dependence of the Q -factor of the cavity was calibrated using a Mn^{2+} – MgO solid solution. The absolute value of the spin susceptibility, χ_{spin} , was determined with reference to the signal of $\text{CuSO}_4 \cdot 5\text{H}_2\text{O}$. In order to investigate the lower temperature, the $\text{Et}_2\text{Me}_2\text{Sb}$ was also measured using an X-band spectrometer ESP-300E (Bruker) (with a cylindrical cavity: TM_{110}) equipped with an Oxford continuous-flow cryostat down to 4.3 K. We confirmed the consistency of the results measured by both equipments. The observed lines are always single Lorentzian down to the lowest temperature except for the angular dependence measurements for aligned crystals (*vide infra*).

Results and discussion

We have performed EPR measurements of $\text{Pd}(\text{dmit})_2$ compounds with a counter cation of Me_4Z (Z = As and Sb) and $\text{Et}_2\text{Me}_2\text{Z}$ (Z = P, As and Sb). Although the structural difference is small among these compounds, the EPR properties are quite different. In this paper, we present the experimental results of the typical three compounds, (1) β' - $\text{Et}_2\text{Me}_2\text{P}[\text{Pd}(\text{dmit})_2]_2$, (2) β' - $\text{Et}_2\text{Me}_2\text{Sb}[\text{Pd}(\text{dmit})_2]_2$ and (3) β' - $\text{Me}_4\text{As}[\text{Pd}(\text{dmit})_2]_2$ (hereafter we abbreviate them as $\text{Et}_2\text{Me}_2\text{P}$, $\text{Et}_2\text{Me}_2\text{Sb}$ and Me_4As , respectively).

$\text{Et}_2\text{Me}_2\text{P}$ exhibits a superconducting transition in the

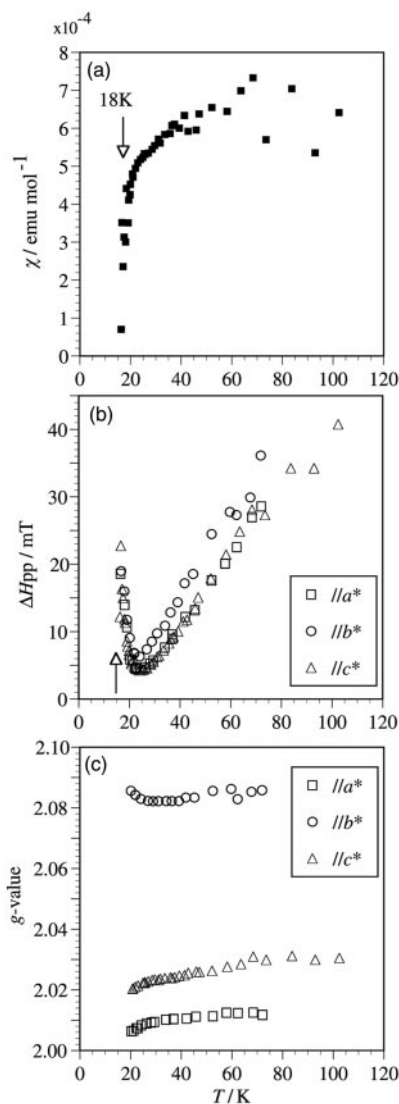


Fig. 1 Temperature dependence of EPR parameters of β' - $\text{Et}_2\text{Me}_2\text{P}[\text{Pd}(\text{dmit})_2]_2$, (a) χ_{spin} determined by EPR intensity, (b) ΔH_{pp} , and (c) g values ($//a^*$ (square), $//b^*$ (circle), $//c^*$ (triangle)).

pressure region of 6.9–10.4 kbar with $T_c = 4.0$ –1.8 K.¹⁰ Measurements of EPR parameters of $\text{Et}_2\text{Me}_2\text{P}$ were performed for 10 aligned crystals. Fig. 1(a) shows the temperature dependence of the spin susceptibility, χ_{spin} , determined by the EPR intensity. The absolute value of $5.0 \times 10^{-4} \text{ emu mol}^{-1}$ at 40 K is almost the same as, or slightly larger than that determined by SQUID magnetometry in a previous report.¹⁰ Scattering of data at high temperatures is due to weak EPR signals associated with huge broadening of the linewidth. Gradual decrease of χ_{spin} below 50 K with a broad hump around 80 K was also observed in the SQUID measurements. Sudden disappearance of the EPR signal below 18 K indicates a phase transition. Fig. 1(b) shows the temperature dependence of the peak-to-peak linewidth, ΔH_{pp} . The ΔH_{pp} decreases as temperature decreases. At low temperatures, divergence of the ΔH_{pp} with a minimum around 20 K was observed, indicating magnetic long-range fluctuation. Hence we concluded that the origin of the phase transition at 18 K is magnetic ordering ($T_N = 18$ K). Fig. 1(c) shows the temperature dependence of the

g -values of $\text{Et}_2\text{Me}_2\text{P}$ when applying the external static field along the orthogonal three axes. The anisotropy of the g -values is huge even in the case of the external field applied in the conduction plane. These features are different from TTF based organic conductors where the in-plane anisotropy of the g -values is small and the g -value shows a maximum when the external field is applied perpendicular to the conducting plane. Detailed analyses of the g -tensor will be discussed in the following section. The g -values are almost temperature independent. The EPR properties of β' - $\text{Et}_2\text{Me}_2\text{As}[\text{Pd}(\text{dmit})_2]_2$ and β' - $\text{Me}_4\text{Sb}[\text{Pd}(\text{dmit})_2]_2$ are very similar to those of $\text{Et}_2\text{Me}_2\text{P}$. Hence we omit these results here. The T_N 's of both compounds were determined as 18 K. The T_N 's determined by EPR measurement in this study are summarized in Table 1. Recently Me_4Sb was found to undergo a superconducting transition under pressure.¹¹ The $\text{Et}_2\text{Me}_2\text{P}$ and Me_4Sb compounds mentioned above show various electronic phases as pressure increases, non-metal \rightarrow superconductor \rightarrow metal \rightarrow insulator. On the other hand, β' - $\text{Et}_2\text{Me}_2\text{Sb}[\text{Pd}(\text{dmit})_2]_2$ exhibits neither superconducting nor second insulating phases even at high pressures.¹⁰ Only a non-metal \rightarrow metal transition was observed as pressure increases. (The $\text{Et}_2\text{Me}_2\text{As}$ compound shows similar pressure dependence. It may be located on its boundary.)

Fig. 2 shows the temperature dependence of the EPR parameters of $\text{Et}_2\text{Me}_2\text{Sb}$. The reliable absolute value of χ_{spin} cannot be estimated because of the small mass of the crystal, but it is almost the same as that of $\text{Et}_2\text{Me}_2\text{P}$. Fig. 2(a) shows the relative temperature dependence of χ_{spin} determined by the EPR intensity. The EPR signal remained down to the lowest temperature, indicating the absence of the antiferromagnetic transition at least down to 4.3 K. χ_{spin} shows almost temperature independent behavior with a slight increase below 10 K. The ΔH_{pp} monotonically decreases as temperature decreases down to the lowest temperature as seen in Fig. 2(b). The absolute values of the ΔH_{pp} for each axis are larger than those of $\text{Et}_2\text{Me}_2\text{P}$. Fig. 2(c) shows the temperature dependence of the g -values of $\text{Et}_2\text{Me}_2\text{Sb}$. Roughly speaking, the g -values of each axis are almost temperature independent, and close to those of $\text{Et}_2\text{Me}_2\text{P}$. As temperature decreases, they gradually decrease.

The third group of compounds, Me_4P and Me_4As , show no metallic behavior even under high pressure.¹⁰ Fig. 3 shows the temperature dependence of the EPR parameters of Me_4As . The abrupt decrease of χ_{spin} and the divergence of ΔH_{pp} around 35 K obviously show the existence of the magnetic order. We determined T_N of the Me_4As compound as 35 K. An abrupt change of the g -values is considered to be an apparent phenomenon due to demagnetization in the proximity of the antiferromagnetic transition. At high temperatures, the g -values show appreciable temperature dependence especially along the b^* axis.

One of the questions that arises from above results is “Why the T_N 's of $\text{Pd}(\text{dmit})_2$ show crucial counter ion dependence?” Recently Rouziere *et al.* discussed variations in the electronic structures in relation to the structural changes and with the influence of the cation on the crystal from the point of view of X-ray diffraction investigation.⁹ Considering the strong dimerization of $\text{Pd}(\text{dmit})_2$, they estimated intermolecular overlap integrals. They show that the electronic degree of dimerization increases as counter cation size becomes larger. The difference of the T_N 's may be due to the degree of dimerization. Actually, there is a trend that compounds with

Table 1 Determined T_N of the β' -type $\text{Pd}(\text{dmit})_2$ compounds

Cation	$\text{Et}_2\text{Me}_2\text{Sb}$	$\text{Et}_2\text{Me}_2\text{As}$	$\text{Et}_2\text{Me}_2\text{P}$	Me_4Sb	Me_4As	Me_4P	Me_4N
T_N	—	18	18	18	35	35	12

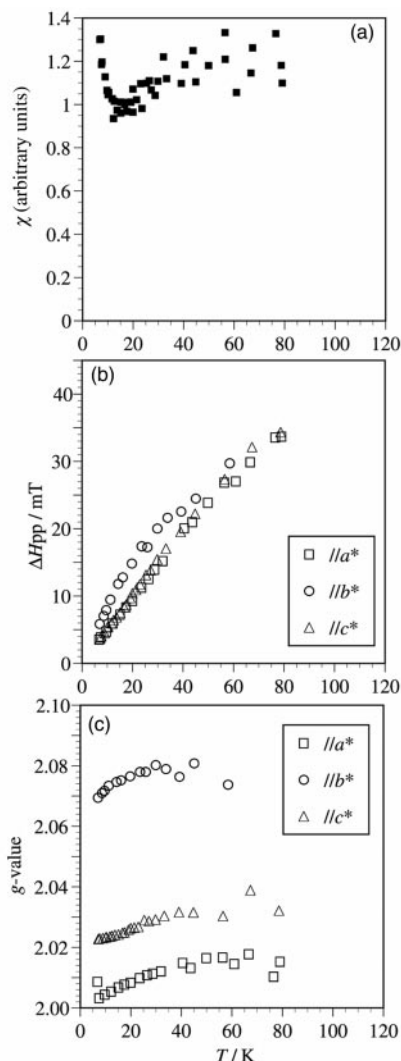


Fig. 2 Temperature dependence of EPR parameters of β' - $\text{Et}_2\text{Me}_2\text{Sb}[\text{Pd}(\text{dmit})_2]_2$, (a) χ_{spin} determined by EPR intensity, (b) ΔH_{pp} , and (c) g values ($//a^*$ (square), $//b^*$ (circle), $//c^*$ (triangle)).

large counter cations possess lower T_N 's. However no linear relationship was found. The counter cation size and dimerization effect are also important for the dimensionality of electronic structure. The HOMO band has two-dimensional character, while the LUMO is one-dimensional. As a result, the dimerization enhances the two-dimensional character of the HOMO through HOMO–LUMO level-crossing. Here we try to consider inter-dimer interaction between stacks. In this paper, we estimated the inter-dimer interaction between stacks as the overlap integral. Fig. 4 shows the relationship of the inter-dimer interaction *versus* the T_N . The parameters, A , B and r , are adopted as those given at room temperature in previous papers.^{3,8,9,12} Here we denote the 'inter'-dimer interaction within stacks normalized 'intra'-dimer interaction as B/A , the 'inter'-dimer interaction between stacks normalized 'intra'-dimer interaction as r/A , and anisotropy of the inter-dimer interaction as r/B . Previous results determined by $^1\text{H-NMR}$, β' - $\text{Me}_4\text{N}[\text{Pd}(\text{dmit})_2]_2$ ($T_N = 12$ K), β' - $\text{Me}_4\text{P}[\text{Pd}(\text{dmit})_2]_2$ ($T_N = 35$ K), β' - $\text{Me}_4\text{N}[\text{Pd}(\text{dmise})_2]_2$ ($T_N = 14$ K) and β' - $\text{Me}_4\text{P}[\text{Pd}(\text{dmise})_2]_2$ ($T_N = 40$ K), are also included in this figure.^{5,6}

We found a close relationship between T_N and the inter-dimer interaction: the T_N seems to decrease as B/A decreases, and r/A increases. It is noted that the T_N decreases as r/B approached 1 from 0.5: the interaction between stacks of $\text{Et}_2\text{Me}_2\text{Sb}$, where no magnetic order was observed down to 4.3 K, is comparable to that within stacks.

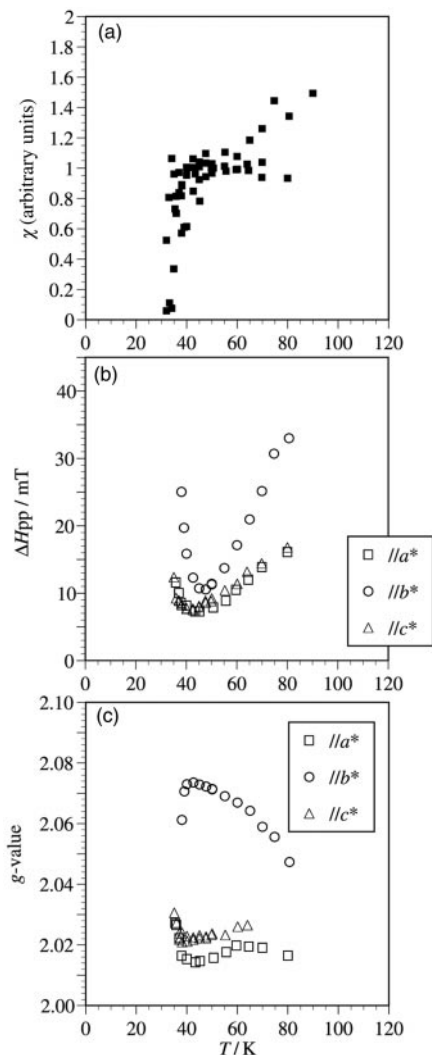


Fig. 3 Temperature dependence of EPR parameters of β' - $\text{Me}_4\text{As}[\text{Pd}(\text{dmit})_2]_2$, (a) χ_{spin} determined by EPR intensity, (b) ΔH_{pp} , and (c) g values ($//a^*$ (square), $//b^*$ (circle), $//c^*$ (triangle)).

Rouziere *et al.* pointed out the possibility of magnetic frustration within conduction layers at low temperature with the anisotropy of the interaction between the $\text{Pd}(\text{dmit})_2$ dimers.⁹ Recently theoretical investigation of effective exchange interactions for dimerized systems was performed by Mori *et al.*¹³ Assuming that the HOMO levels are dominant for magnetic interactions, the calculated T_N and magnitude of local moments for $\text{Pd}(\text{dmit})_2$ are qualitatively in agreement with EPR and $^1\text{H-NMR}$ results.

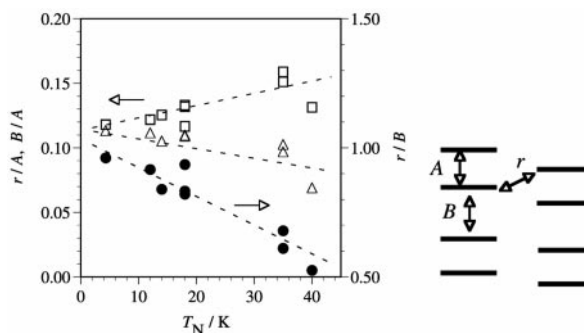


Fig. 4 Relationship of the inter-dimer interaction *versus* the T_N . The parameters, A , B and r , which are schematically shown in the insets, are the same in refs. 3,8,9,12. $\triangle = r/A$ (H-H), $\square = B/A$ (H-H), $\bullet = r/B$. The broken line is a guide to the eye.

Lastly we present the results of the g -tensor analyses, and discuss the symmetry of the wave-function. We performed angular dependence of the g -values of $\text{Et}_2\text{Me}_2\text{P}$ at 25 K in order to perform the g -tensor analyses to provide significant information. When the static magnetic field was applied in the midway angle within the a^*c^* plane, the resonance line was split into two. The ratio of the relative intensity is approximately 6:4. Since the crystal structure is monoclinic and we used 10 aligned crystals for the measurement, two arrangements are possible when we put the a^*c^* plane of the crystals parallel to the EPR sample stage. Assuming this, we can evaluate the principal values and axes of the g -tensor by least squares fit to the measured data assuming an anisotropic g -value.

Fig. 5 shows the determined principal axes and values on the actual $\text{Pd}(\text{dmit})_2$ arrangements. One of the principal axes, g_1 , lies along the b -axis, which is roughly the direction of the molecular short axis. The principal axis, g_2 , lies along the molecular long axis, and g_3 is close to the direction normal to the molecular plane. The principal axes are well explained as the average of the molecular axes of $\text{Pd}(\text{dmit})_2$ radicals with solid crossing columns: we can treat the directions of them as in the framework for conventional organic conductors. On the other hand, the principal values of $\text{Pd}(\text{dmit})_2$ show characteristic features. The large shift from g_e of the g_1 and g_2 are remarkable, although the small shift of g_3 is explained by the fact that HOMO and/or LUMO are mainly composed of orbitals elongated in the z direction. Considering the huge shift of g_1 , it seems likely that the $\text{Pd } d_{3z^2-r^2}$ orbital is also composed of the wave-function besides the p_z orbital of C and S. It is noted that the principal value shows its maximum for the molecular short axis, while the maximum principal values of TTF derivatives are along the molecular long axes. This fact suggests that there is only a small contribution of the $\text{Pd } d$ orbital along the molecular long axis. However, an isolated $\text{Pd}(\text{dmit})_2$ possesses a HOMO without d contribution because of its symmetry according to the extended Hückel molecular orbital calculation. Moreover, the average of the principal values, $\langle g_{\text{AV}} \rangle$ (2.038), of β' - $\text{Et}_2\text{Me}_2\text{P}[\text{Pd}(\text{dmit})_2]_2$ does not agree with that of a 1:1 radical, $\text{Bu}_4\text{N}[\text{Pd}(\text{dmit})_2]$ (Bu = butyl) solution, $\langle g \rangle$ (=2.0191). The observed g -tensor cannot be explained by that of an isolated $\text{Pd}(\text{dmit})_2$ molecule.

For conventional organic conductors, the principal values and axes of the crystal are well explained by taking into account the principal values and the axes of the g -tensor of the radical and the geometry of the molecular stacking in the crystal.¹⁴ The above consideration is also available even in the paramagnetic

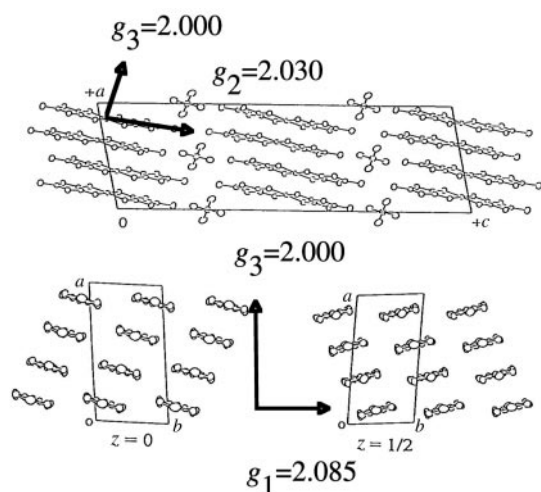


Fig. 5 Determined principal axes and values on the actual crystal structure.

states of an antiferromagnet with strong “dimer” structure, κ - $(\text{BEDT-TTF})_2\text{Cu}[\text{N}(\text{CN})_2]\text{Cl}$.¹⁵ Recent first-principle calculations by Miyazaki *et al.* including the actual dimer effect suggest that the HOMO of $\text{Pd}(\text{dmit})_2$ has appreciable contributions from the $\text{Pd } d_{3z^2-r^2}$ orbitals.¹⁶ This expectation coincided with the EPR results. It is likely that the discrepancy of the g -tensor from the isolated radical is due to the deformation of the wave-function with the strong dimer structure of the $\text{Pd}(\text{dmit})_2$ system.

In conclusion, we investigated the low temperature electronic states and determined the T_N 's of the series of β' - $\text{Pd}(\text{dmit})_2$ compounds. The EPR ΔH_{pp} and T_N 's show crucial counter ion dependence, and we found a close relationship between the T_N 's and ‘inter’-stack interaction. It is proposed that possible frustration of local moments on triangle dimers reduces the T_N 's and magnitude of the local moments. The EPR g -values of $\text{Pd}(\text{dmit})_2$ are found to be beyond one radical description; we should consider the wave-function $[\text{Pd}(\text{dmit})_2]_2$ supramolecules. These experimental facts from the view point of magnetic investigation are evidence that compounds of this family are Mott–Hubbard insulators with a dimer as a unit. Recently we succeeded in synthesizing ^{13}C substituted $\text{Pd}(\text{dmit})_2$ molecules, and started ^{13}C -NMR measurements. Further ^{13}C -NMR investigations are in progress.

Acknowledgements

We thank S. Rouziere, M. Mori and K. Yonemitsu for useful discussions. Thanks are also due to T. Miyazaki for kindly supplying us with the calculation results. This work was carried out as a part of “Research for the Future project”, JSPS-RFTF97P00105, supported by Japan Society for the Promotion of Science, and was supported by the Grant-in-Aid for Scientific Research on Priority Area “Metal-assembled Complexes” (No. 10149245) from the Ministry of Education, Science, Sports and Culture of Japan.

References

- For a review see: P. Cassoux, L. Valade, H. Kobayashi, R. A. Clark and A. E. Underhill, *Coord. Chem. Rev.*, 1991, **110**, 115.
- A. Kobayashi, H. Kim, Y. Sasaki, K. Murata, R. Kato and H. Kobayashi, *J. Chem. Soc., Faraday Trans.*, 1990, **86**, 361.
- R. Kato, Y.-L. Liu, S. Aonuma and H. Sawa, *Solid State Commun.*, 1995, **98**, 1021.
- (a) E. Canadell, S. Ravy, J. P. Pouget and L. Brossard, *Solid State Commun.*, 1990, **75**, 633; (b) E. Canadell, I. E.-I. Rachidi, S. Ravy, J. P. Pouget, L. Brossard and J. P. Legros, *J. Phys. Fr.*, 1989, **50**, 2967; (c) H. Tajima, T. Naito, M. Tamura, A. Kobayashi, H. Kuroda, R. Kato, H. Kobayashi, R. A. Clark and A. E. Underhill, *Solid State Commun.*, 1991, **79**, 337.
- Y. Tsuchiya, T. Nakamura, T. Takahashi, Y.-L. Liu, H. Sawa and R. Kato, *Synth. Met.*, 1997, **86**, 2117.
- K. Seya, Y. Kobayashi, T. Nakamura, R. Kato, A. Kobayashi and H. Iguchi, *Synth. Met.*, 1995, **70**, 1043.
- S. Aonuma, H. Sawa and R. Kato, *Synth. Met.*, 1997, **86**, 1881.
- R. Kato, Y.-L. Liu, Y. Hosokoshi and S. Aonuma, *Mol. Cryst. Liq. Cryst.*, 1997, **296**, 217.
- S. Rouziere, J.-I. Yamaura and R. Kato, *Phys. Rev. B*, 1999, **60**, 3113.
- R. Kato, Y. Kashimura, S. Aonuma, N. Hanasaki and H. Tajima, *Solid State Commun.*, 1998, **105**, 561.
- M. Tamura, A. Eguchi, Y. Nishio and K. Kajita, Annual Meeting of the Physical Society of Japan, Hiroshima, March 1999.
- R. Kato, Y.-L. Liu, H. Sawa, S. Aonuma, A. Ichikawa, H. Takahashi and N. Mori, *Solid State Commun.*, 1995, **94**, 973.
- (a) M. Mori, K. Yonemitsu and H. Kino, *Synth. Met.*, 1999, **103**, 1883; (b) M. Mori, K. Yonemitsu and H. Kino, *Mol. Cryst. Liq. Cryst.*, 2000, **341**, 549.
- T. Nakamura, T. Nobutoki, T. Takahashi, G. Saito, H. Mori and T. Mori, *J. Phys. Soc. Jpn.*, 1994, **63**, 4110.
- W. Minagawa, T. Nakamura and T. Takahashi, *Synth. Met.*, 1997, **85**, 1565.
- T. Miyazaki and T. Ohno, *Phys. Rev. B*, 1999, **59**, R5269.